J Mol Model (2012) 18:2645–2652
DOI 10.1007/s00894-011-1289-8

ORIGINAL PAPER

Aminoglycoside induced nephrotoxicity: molecular modeling studies of calreticulin-gentamicin complex

Gururao Hariprasad · Manoj Kumar · Komal Rani · Punit Kaur · Alagiri Srinivasan

Received: 28 June 2011 / Accepted: 20 October 2011 / Published online: 16 November 2011

Abstract Gentamicin is a member of aminoglycoside group of broad spectrum antibiotics. It impairs protein synthesis by binding to A site of the 30S subunit of bacterial ribosomes. One of the main side effects of this drug is nephrotoxicity. The drug is known to bind to calreticulin, a chaperone essential for the folding of glycosylated proteins. We provide a detailed structural insight of the calreticulin-gentamicin complex by molecular modeling and the binding of the drug in the presence of explicit solvent was analyzed by molecular dynamics simulation. The gentamicin molecule binds to the lectin site of the calreticulin and lies in the concave channel formed by the long beta sheets. It makes interactions with residues Tyr109, Asp125, Asp135, Asp317 and Trp319 which are crucial for the chaperone function of the calreticulin. The superimposing of the modeled complex with the only available crystal structure complex of calreticulin with a tetrasaccharide (Glc_1Man_3) shows interesting features. First, the rings of the gentamicin occupy the positions of glucose and the first two mannose sugars of the tetrasaccharide molecule. Second, the oxygen atoms of the glycosidic linkage of these two ligands have a positional deviation of 1.3 Å. The predicted binding constant of 16.9 μM is in accordance with the previous kinetic study experiments. The details therefore, strongly implicate gentamicin as a competitive inhibitor of sugar binding with calreticulin.

Keywords Adverse drug reaction · Molecular modeling

Abbreviations

ABNR	Adopted basis set Newton-Raphson
CHARMM	Chemistry at Harvard molecular mechanics
PROCHECK	Protein structure check
PDB	Protein Data Bank
r.m.s	root mean square
MMFF	Merck molecular force field

Introduction

Aminoglycosides have been very valuable in numerous clinical scenarios despite their toxic effects in the human body [1, 2]. Gentamicin is an aminoglycoside antibiotic, used for the treatment of gram-negative bacillary infections. It binds to A-site of the bacterial 30S subunit ribosomes resulting in the misreading of the mRNA and/or premature termination of protein synthesis [3]. Structurally, an aminoglycoside is a glycosylated molecule which also has amino substitution on the glycosyl moiety. Gentamicin is composed of three rings: ring I is purpurosamine (G1), ring II is deoxystreptamine (G2) and ring III is gentosamine or garosamine (G3) (Fig. 1). Gentamicin is a basic compound with a molecular weight of 477.6.

It was found recently that 209 of the 360 patients receiving aminoglycoside therapy in an intensive care unit developed aminoglycoside induced nephrotoxicity [4]. Though there are a number of theories relating to the possible mechanisms of nephrotoxicity [5–10], some of the

Gururao Hariprasad and Manoj Kumar have contributed equally in the paper

Electronic supplementary material The online version of this article (doi:10.1007/s00894-011-1289-8) contains supplementary material, which is available to authorized users.

G. Hariprasad · M. Kumar · K. Rani · P. Kaur · A. Srinivasan (✉)
Department of Biophysics,
All India Institute of Medical Sciences,
110029 New Delhi, India
e-mail: srini@aiims.ac.in

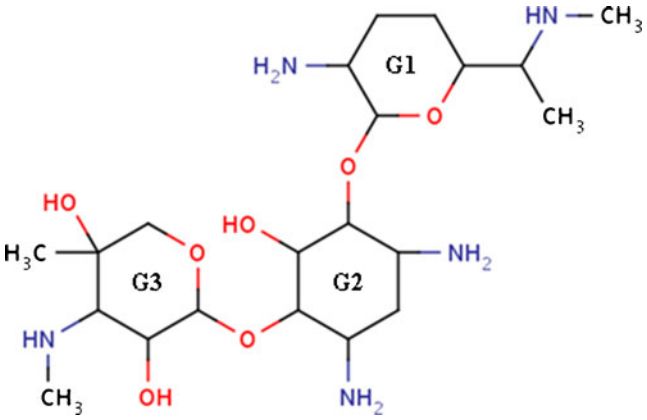

Fig. 1 Chemical structure of the aminoglycoside, gentamicin at neutral state. The 2D chemical structure was drawn using Symyx Draw 3.3

recent studies relate to the chaperonic proteins in the kidney. The drug gentamicin inhibits calreticulin, a chaperonic protein known to assist the folding of glycoproteins [11]. Inhibition of chaperone proteins will result in the accumulation of unfolded proteins. Unfolded protein response can in turn induce apoptosis. We report here the modeled structure complex of calreticulin with gentamicin. The corollaries of these results will be that (1) identification of the interaction partners of a drug will predict the adverse drug reactions and (2) the structural information will help to improve the design of drugs with less toxicity and better therapeutic efficacy [12].

Materials and methods

Sequence analysis

Protein sequences of calreticulin from mouse, rat, rabbit, human, pig and cow were taken from National Centre for Biotechnology Information. The sequences were aligned using CLUSTALW available at ExPASY (http://expasy.org/tools/#proteome) and analyzed for the conservation pattern.

Modeling studies

The crystal structure complex of mouse calreticulin with tetrasaccharide (PDB Id: 3O0W) [13] was taken as the starting point for the docking analysis. All computational analysis for the docking was done using in house Discovery Studio, version 2.0 (DS 2.0) [14].

Receptor preparation

The water molecules, tetrasaccharide and ions were removed from the complex. The hydrogen atoms were added to the protein and their positions were optimized using all atom CHARMm (version-c33b1) force field [15, 16] with adopted basis set Newton Raphson (ABNR) minimization protocol in DS 2.0 until the r.m.s gradient was less than 0.05 kcal mol^{-1} $Å^{-1}$. The hydrogen optimized calreticulin was defined as the receptor. The binding site was defined as the volume of the tetrasaccharide and edited further to accommodate all the interacting residues of calreticulin. The input site sphere was defined over the binding site with a radius of 5 Å from the center of the binding site. The side-chains of the residues in the binding site within the radius of the sphere were taken to be flexible during refinement of post-docking poses. The receptor with the defined binding site was used for the docking studies.

Ligand preparation

The coordinates of gentamicin were taken from its crystal structure complex with ribosome of *Escherichia coli* (PDB id: 2QBA). The ionization state of gentamicin at pH 7 was calculated using 'prepare ligand' protocol available in DS 2.0. The force field parameters were taken from Merck molecular force field [17]. The structure of the gentamicin was minimized to obtain its lowest energy conformation using the above mentioned minimization protocol. The minimized gentamicin was used as the ligand for the docking studies with mouse calreticulin.

Docking and scoring

LigandFit [18] docking protocol of DS 2.0 was used for the docking of gentamicin into the binding pocket of calreticulin. The LigandFit docking algorithm combines a shape comparison filter with a Monte Carlo conformational search to generate docked poses consistent with the binding site shape. These docked poses are refined by rigid body minimization of the ligand with respect to the grid-based calculated interaction energy using the Dreiding force field [19]. The docked poses are ranked according to Dock score which is the negative sum of interaction energy and internal energy of the ligand. The pose with the highest Dock score [18] was taken as the most probable binding mode and further scored with empirical scoring functions for the quantitative estimation of binding strength (K_d). Among empirical scoring functions, the calculated K_d value based on LigScore 1 [20] was closest to the experimentally determined binding affinity for gentamicin. The K_d value was calculated using formula: LigScore 1=−log K_d. LigScore 1 calculates the free energy of binding for a given protein-ligand complex of known 3-D structure using empirical parameters: van der Waals descriptors based on Dreiding force field using softened (6–9) Lennard-Jones

potential, buried polar surface area between ligand and receptor as well as total surface area of ligand and receptor.

Since the receptor protein was kept fixed during docking, the docked poses were further minimized using all-atom CHARMm (version c33b1) force field with the help of smart minimization method (steepest descent followed by conjugate gradient) until r.m.s. gradient for potential energy was less than 0.05 kcal mol^{-1} $Å^{-1}$ and the interaction energy was calculated. All the contributions of interactions of non-electrostatic origin were calculated as steric energy using Lennard-Jones potential. The electrostatic energy was calculated using Coulomb's potential with implicit solvent model, distance dependent dielectric, in case of absence of water solvent.

Validation of docking methodology

The docking methodology was first verified by extracting the ligand (tetrasaccharide) from its complex of mouse calreticulin (PDB ID: 1O0W) and then docked into the binding site of mouse calreticulin. The tetrasaccharide was extracted, its ionic state was calculated at pH 7, MMFF94 parameters were assigned, hydrogens were added and their positions were optimized using ABNR minimization algorithm until the r.m.s gradient is less than 0.05 kcal mol^{-1} $Å^{-1}$. It was then docked into the binding site of the calreticulin and compared with its crystal structure conformation. The accuracy of the docking prediction was measured by the positional r.m.s deviation of heavy atoms of tetrasaccharide between the docked pose and the crystal conformation. The binding constant (K_d) of the docked ligand was calculated using LigScore 1 and compared with its experimental binding data.

Molecular dynamics simulation

The stability of the binding of the gentamicin to calreticulin was analyzed by molecular dynamics (MD) simulation of calreticulin-gentamicin complex in the presence of explicit solvent molecules. The all atom CHARMm (version-c33b1) force field parameters were assigned to the calreticulin while MMFF94 force field parameters were assigned to gentamicin. The minimized calreticulin-gentamicin complex was hydrated with TIP3, using "explicit spherical boundary with harmonic restraint" solvation protocol available in DS 2.0. The hydrated protein-ligand complex was minimized in two steps. First, the bad contacts were removed between solvents and the protein-ligand complex using the steepest descent minimization algorithm with convergent criteria of <0.1 kcal mol^{-1} $Å^{-1}$ r.m.s gradient. It was followed by minimization employing conjugate gradient algorithm with convergent criteria of less than 0.05 kcal mol^{-1} $Å^{-1}$ r.m.s gradient to refine the solvated complex. To start with the MD simulation, temperature of the system was raised from 50 to 300 K (50 K, 100 K, 150 K, 200 K, 250 K and 300 K) for 5 ps at each temperature. The system was then equilibrated for 1000 ps at the target temperature of 300 K using 'adjust velocity frequency' method. Finally, the production run was carried out for 1000 ps for the canonical ensemble (NVT) using Leapfrog Verlet dynamics integrator and Brendsen temperature coupling bath. In all three stages (heating, equilibration and production) of simulation, a time step of 1 fs was used.

Results and discussion

Sequence and structural analysis of calreticulin

Sequence analysis shows the mouse calreticulin to have an identity of at least 93% with other mammalian group species including humans (Fig. SI). The cysteine residues at the positions 105, 137 and 163 are conserved among all the species. The signal sequence for endoplasmic reticulum localization [21] and sugar binding residues are conserved in all the sequences justifying the use of mouse calreticulin crystal structure as the template for the modeling studies. The mouse calreticulin structure has been described in detail by Kozlov and his group very recently [13]. The structure of calreticulin is comprised of four α-helices and 13 β-strands interconnected by loops. The cysteines 105 and 137 connect to form a disulfide bond.

Validation of docking and scoring function

The docking methodology has been validated by docking the tetrasaccharide, Glc_1Man_3, to calreticulin and comparing the modeled structure complex with the crystal structure complex (PDB Id: 3O0W). The ligand conformations of the sugars in the two complexes have a positional r.m.s deviation of 1.1 Å (Fig. 2) establishing the validity of the docking method used. The steric, electrostatic and the total interaction energies of the two complexes are comparable (Table 1). The calculated binding constant (K_d) of the docked sugar Glc_1Man_3 to calreticulin based on LigScore I is 2.34 μM and is comparable with the experimentally determined values (Table 2). This result establishes the predictive power of LigScore I in combination of LigandFit docking function to estimate the binding constant of gentamicin into the binding site of calreticulin.

Calreticulin-gentamicin complex

Gentamicin was docked to the lectin binding site, as it is known to bind to this site on calreticulin [11]. Molecular docking studies show gentamicin occupying a concave

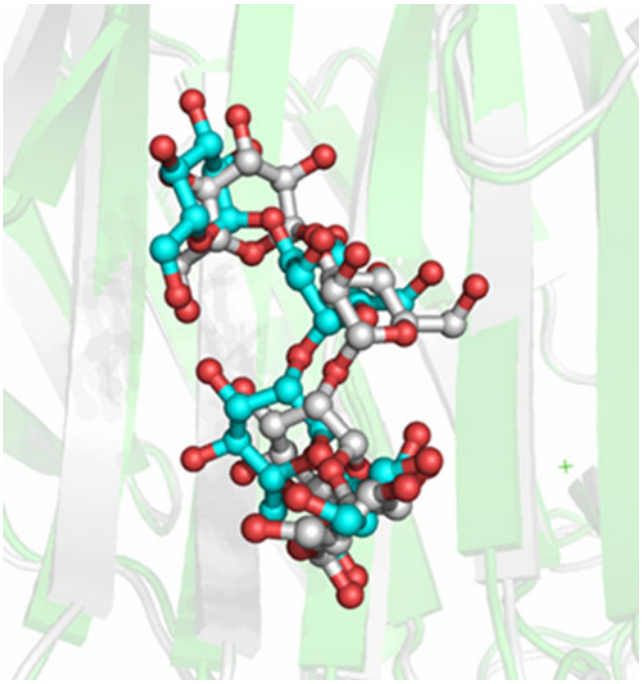

Fig. 2 Docked and crystal structure (PDB Id: 3O0W) conformations of the tetrasaccharide, α - D - glucopyranose - (1 → 3) - α - D - mannopyranose - (1 → 2) - D – mannopyranose - (1 → 2) – D - mannose (Glc1Man3) in the cavity of mouse calreticulin The crystal ligand is shown in silver rendering and the docked ligand is shown in cyan rendering

surface formed by the β-sheets (Fig. 3). This site is also the recognition site for the sugar moiety of unfolded glycosylated proteins. Gentamicin makes many interactions including seven hydrogen bonds with four residues of calreticulin (Table 1 and Fig. 4). The hydrogen bonds are: Cys105 S ··· N G3=3.2 Å, Tyr109 OH ··· N G1=2.5 Å, Tyr109 OH ··· O G2=3.3 Å, Asp125 Oδ1 ··· N G2=3.0 Å, Asp125 Oδ1 ··· N G1=3.1 Å, Asp125 Oδ2 ··· N G2=2.9 Å and Asp317 Oδ2 ··· N G1=2.6 Å. The hydrogen bonding residues Cys105 and Asp317 are from the β-sheets which are the floor of the binding site, Tyr109 is from the short loop connecting the third and fourth β-strands and Asp125 is from the loop connecting the fourth and the fifth β-strands. It is very likely that the participation of each of the gentamicin rings in at least one hydrogen bond is responsible for the stability of the ligand at the current conformational position. The interaction energy estimated for calretculin-gentamicin complex is lower in comparison to the calreticulin-tetrasaccharide complex. While the steric energy is approximately the same, the electrostatic energy is lower by 24 kcal mol^{-1} in the case of gentamicin (Table 1). This is because of the charged state of gentamicin (+2) at pH 7 compared to the neutral tetrasaccharide. However, the number of hydrogen bonds and van der Waals interactions in the two complexes are approximately the same. The interaction energy of the calreticulin-gentamicin complex is indicative of the favorable enthalpy parameters for binding of gentamicin.

Molecular dynamic studies of the calreticulin gentamicin complex

The effect of the solvent on the binding of gentamicin was studied in detail by a MD simulation of a fully hydrated calreticulin model. The total energy and temperature were found to remain steady with little fluctuation during the production stage of 1 ns. The r.m.s deviation of the conformations from production stage to the end of equilibration varies from 0.07 Å to 0.073 Å. The interaction energy shows a 40 kcal mol^{-1} variation during simulation (Table 3). In comparison to the non-solvated complex, the solvated complex shows gentamicin with a much lower docked energy. The snap shots of the dynamics trajectory at 0, 200, 400, 600 800 ps and 1000 ps of the production run show that ligand and interacting residues are stable during simulation (Fig. 5). At the end of the simulation, water molecules are seen in the vicinity of the ligand. These water molecules make 13 direct contacts with gentamicin and participate in six water mediated hydrogen bonds between

Table 1 Comparative structure analyses of calreticulin complexes

No.	Structure	Methodology used	Total energy (kcals/mol)			r.m.s.d of docked ligand from the crystal complex ligand	Contacting residues of the protein with the ligand (residues making H bonded interactions are shown in bold)
			Stearic	Electrostatic	Total		
1	Calreticulin complex with tetrasaccharide	Crystallization (PDB Id: 1O0W)	−34.3	−45.7	−80.00	-	F74, **G107, Y109,** K111, **G124**, **Y128, D135, H145,** I147, **N154, D317,** L318, W319
2	Calreticulin complex with tetrasaccharide	Docking validation (This study)	−32.7	−49.6	−82.31	1.1 Å	**G107,** Y109**, K111**, **Y128,** M131**, D135,** I147, **D317,** L318, W319.
3	Calreticulin with the antibiotic gentamicin	Docking (This study)	−33.4	−73.7	−107.1	-	F74**, C105,** G106, G107**, Y109**, K111, G124, **D125**, C132, 136, D135, **D317,** W319, V321

Table 2 Binding affinities of ligands with calreticulin

Ligand	K_d (μM)	Reference
Tetrasaccharide	0.7	[13]
Tetrasaccharide	0.7	[25]
Tetrasaccharide	2.0	[26]
Tetrasaccharide	2.34	This study
Gentamicin	384	[11]
Gentamicin	16.9	This study

the residues and the ligand (Fig. 6). It is thereby clear that water molecules further stabilize the complex. This also explains the significant decrease in the total interaction energy of the complex in the presence of solvent.

As the hydrogen bond formation plays a key role in the affinity of a ligand to the protein, these interactions were closely monitored during the MD simulations and compared with the conformation before the start of the simulation (Fig. 7). There is a conformational change in the position of the gentamicin ligand with an angular rotation at the second equatorial oxygen to attain the stability and optimize the interaction as compared to the start of the simulation. The reasons for the movement of the ligand may be two fold. Firstly, there are a total of 13 water molecules of

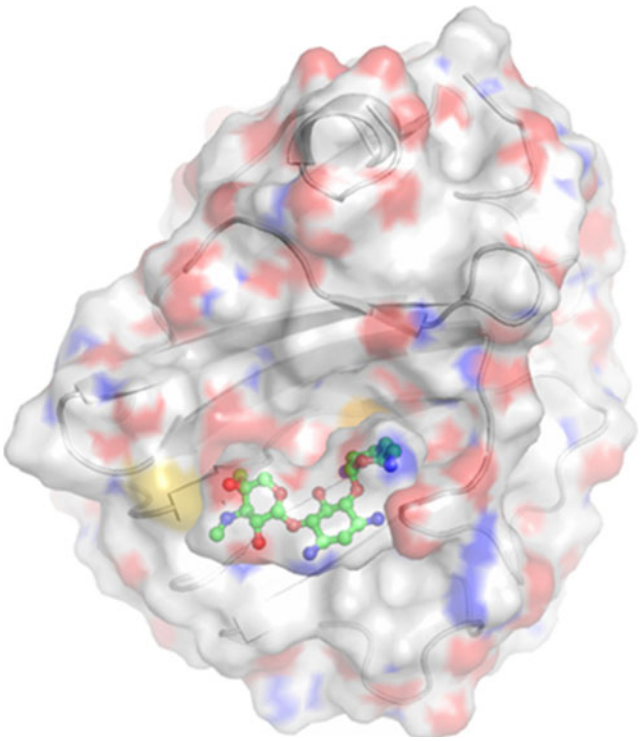

Fig. 3 A GRASP model of calreticulin with the docked ligand gentamicin in ball and stick representation. Surface electric potential of both calreticulin and gentamicin is shown in transparency. The ribbon diagram of the calreticulin shows the floor of the cavity formed by the β-strands

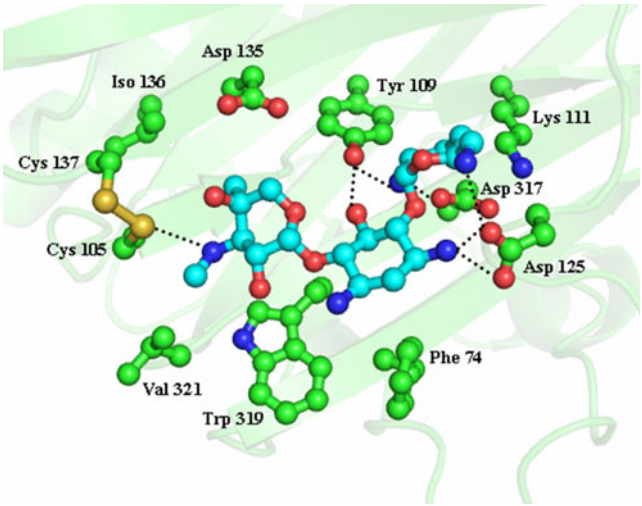

Fig. 4 Ball and stick representations showing the conformation of gentamicin within the cavity of the calreticulin. The calreticulin residues interacting with the gentamicin are shown. Hydrogen bonding is indicated by dotted line

the solvent that form hydrogen bonds with gentamicin. Secondly, there are two major conformational changes in the side chains of the residues at the binding site. They are (1) angular and rotational movement around the Cβ atom of Asp125 to facilitate (a) a direct hydrogen bond formation between Asp125 Oδ2 ··· G2 N=2.8 Å, (b) a water mediated hydrogen bonded interaction between the same two atoms and (c) a water mediated hydrogen bonded interaction between Oδ1 and G2N. A water mediated hydrogen bonded interaction is also seen between main chain oxygen of Asp125 and G1N and (2) angular movement at the Cγ atom of Asp135 to facilitate the hydrogen bond formation between Asp135 Oδ2 ··· G3O=2.8 Å and a water mediated interaction between the same two atoms. The final conformation of gentamicin after simulation looses a hydrogen bond with main chain atom of Cys105 and gains a hydrogen bond with Asp135. In addition to this hydrogen bonded interaction, there are van der Waals contacts at the binding site with the side chains of Trp319, Phe74 and Cys105. The amine group of G3 ring is in close vicinity to the sulfydryl group of Cys105 which is very crucial for the chaperone activity by calreticulin [13]. It is interesting to note that in the calreticulin-sugar complex, Asp125 residue makes water mediated hydrogen bonds with oligosaccharide through ordered water molecules.

Gentamicin as a competitive inhibitor

Calreticulin has a lectin site that binds to the oligosaccharide-containing (Glc1Man5–GlcNAc2) folding intermediates of nascent proteins [22, 23]. Previous substrate specificity studies have reported that the terminal glucose residue of these oligosaccharides is particularly important for recogni-

Table 3 Fully hydrated dynamics simulation results of calreticulin and gentamicin complex

Time (ps)	Docked energy of the ligand (kcal/mol)			Contacting residues (upto 4.0 Å) (hydrogen bonded residues are highlighted in bold)	r.m.s deviation (Å)
	Stearic	Electrostatic	Total		
0	−47.9	−192.1	−240.0	F74, C105, G106, G107, **Y109**, G124, **D125**, **D135**, **D317,** W319, V321	-
200	−42.9	−174.6	−217.5	F74, C105, G106, G107, **Y109**, G124, **D125**, **D135**, **D317,** W319	0.072
400	−49.6	−157.4	−207.1	F74, C105, G106, G107, **Y109**, K111, G124, **D125**, **D135**, **D317,** W319	0.070
600	−48.3	−186.4	−234.7	F74, C105, G106, G107, **Y109**, G124, **D125**, **D135**, **D317,** W319, V321	0.069
800	−45.1	−155.0	−200.1	F74, C105, G106, G107, **Y109**, G124, **D125**, **D135**, **D317,** W319, V321	0.073
1000	−42.5	−194.7	−237.2	F74, C105, G106, G107, **Y109**, G124, **D125**, **D135**, **D317,** W319	0.073

tion by calreticulin [22–24]. The recent structure complex of the calreticulin with the tetrasaccharide confirms the same. The superimposing of calreticulin-gentamicin model complex with available crystal structure complex of calreticulin with the tetrasaccharide (Glc1Man4) (PDB id: 3O0W) shows many interesting features. The purosamine, deoxystreptamine and gentosamine rings of the gentamicin occupy the positions of the glucose and the first two mannose sugars of the tetrasaccharide molecule (Fig. 8). The two oxygens of the glycosidic linkages of both the drug and the sugar have a positional deviation of 1.3 Å and 1.4 Å indicating the binding similarity between the drug gentamicin and tetrasaccharide. The comparative analysis of complexes shows common mode of interactions. Seven residues: Phe74, Tyr109, Lys111, Gly124, Asp135, Asp317 and Trp319 are common in the interactions of calreticulin complexes with gentamicin and the tetrasaccharide. Mutagenic experiments have established that the residues Tyr109, Asp125 and Asp 317 are essential for carbohydrate binding [25–27]. The model structure of calreticulin-gentamicin complex shows that these three residues form hydrogen bonds with gentamicin. The structure of calreticulin-tetrasaccharide complex indicates the presence of hydrogen bond between gentamicin and residues Tyr109 and Asp317 [13]. The calreticulin mutant Y109F did not show any binding indicating the important role of the hydroxyl side chain of Tyr109 in carbohydrate binding [28]. In the present model, the hydroxyl group of Tyr109 forms two hydrogen bonds with hydroxyl group of G2 ring and amine group of G1 ring. Similarly, Asp317 forms a hydrogen bond with amine group of G1 ring of gentamicin. In addition, Asp125 forms hydrogen bonds with amine group of G2 ring and second amine group of G1 ring. Mutants W319I and W319A show reduced carbohydrate binding indicating the importance of this residue [27]. The crystal structure of calreticulin-tetrasaccharide complex shows the presence of hydrophobic contacts between its side chain and terminal mannose sugar [13]. Similarly, the side chain Trp319 shows 11 van der Waals interactions with gentamicin. Also, the counterparts of the calreticulin residues Tyr109 and Lys111 in calnexin are known to participate in sugar binding [29]. The modeled

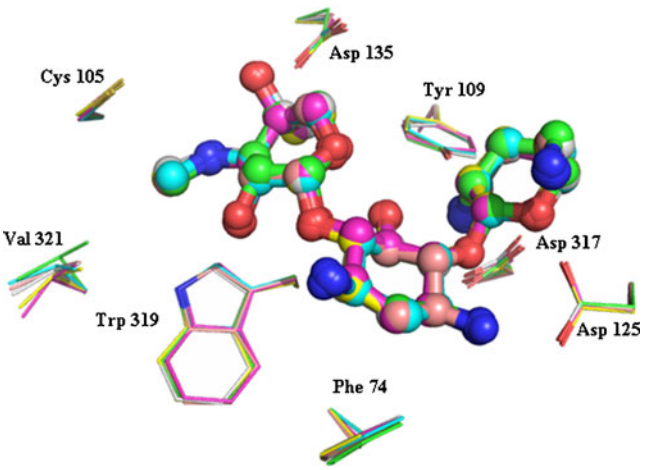

Fig. 5 Molecular dynamics trajectory for the calreticulin and gentamicin complex. Snapshots of the gentamicin and the lectin site residue conformers extracted from the production dynamics trajectory at the time intervals of 0, 200, 400, 600, 800 and 1000 ps. The gentamicin is shown in thick stick rendering and the residues are shown as thin sticks

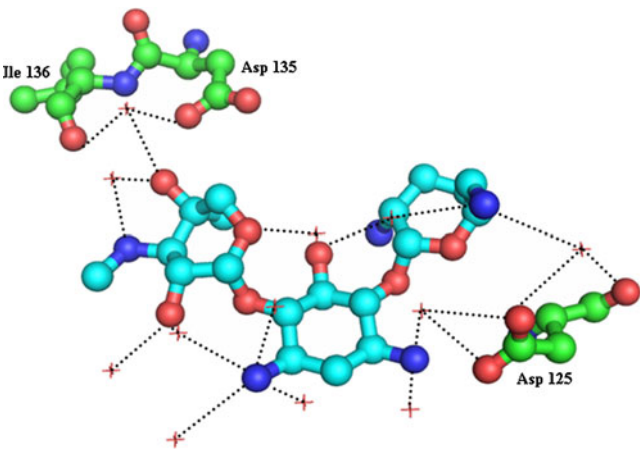

Fig. 6 Water molecules seen in the vicinity of the ligand at the end of molecular dynamics. Hydrogen bonded interactions of water and water mediated interactions of the protein residues with gentamicin are shown. The hydrogen bonding is shown as black dotted lines

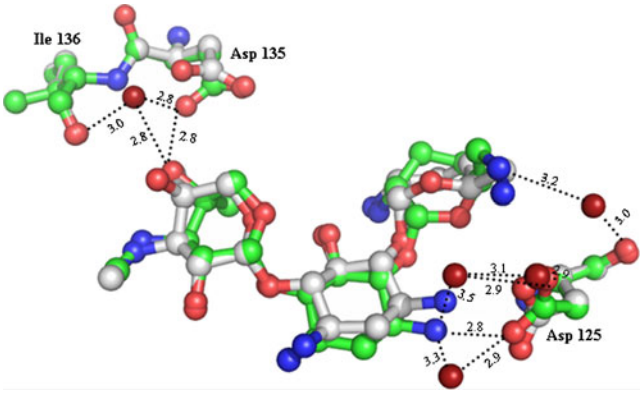

Fig. 7 Superimposition of the residues and ligand conformations (**1**) before (silver rendering) and (**2**) at the end of dynamics simulation with the water molecules (green rendering). The water molecules are shown in brick red. The hydrogen bonding seen at the end of the dynamics study is shown in black dotted lines. The distances (Å) of the hydrogen bonds are shown adjacent to the dotted lines

calreticulin-gentamicin complex shows hydrophobic interactions between the long alkyl part of Lys111 side chain and G1 ring of gentamicin. Similar interactions for the methylene groups of arginine have been proposed earlier [30]. The methyl group on G3 ring of gentamicin has van der Waals interaction with side chain of Val321. However, tetrasaccharide does not interact with Val321. This may be due to the absence of the methyl group on tetrasaccharide. The structural details provided by the modeling study indicate that the pattern of interactions between calreticulin-tetrasaccharide crystal complex is similar to calreticulin-gentamicin complex. Moreover, the predicted binding constant of gentamicin (16.9 μM) is of the same order of a substrate like tetrasaccharide for calreticulin (Table 2). These results point out that gentamicin could be a competitive inhibitor of lectin binding site of calreticulin.

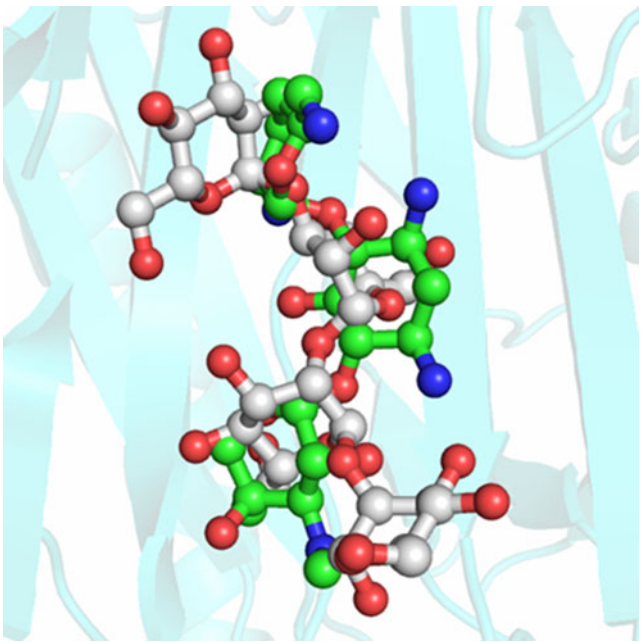

Fig. 8 Superimposition of the docked ligand gentamicin and the crystal structure ligand tetrasaccharide (PDB Id: 3O0W) in the cavity of lectin of the calreticulin molecule. Gentamicin is shown in green rendering and the sugar is shown in silver rendering

The endoplasmic reticulum is the main sub-cellular location of calreticulin [25]. We propose that competitive inhibition of calreticulin by gentamicin results in the accumulation of unfolded protein in the endoplasmic reticulum. We discuss below the implications of this hypothesis. The accumulation of the unfolded proteins in the endoplasmic reticulum lumen in turn induces endoplasmic reticulum stress [31–34]. It is known that gentamicin induces markers of endoplasmic reticulum stress in rat kidneys [35]. Unfolded protein response, a well-conserved adaptive response, can eventually trigger apoptosis if the stress is severe or prolonged as is the case with gentamicin administration [36, 37]. Unfolded protein responses could be manifold: altered regulation of gene expression, oxidative stress, apoptosis etc. The mechanism of gentamicin interfering with the substrate binding of chaperones leading to toxicity is further supported by the observations of inhibition of HSP73 and HSP70 by gentamicin [38, 39]. Gentamicin inhibits HSP70-assisted protein folding by interfering with substrate recognition [39]. Establishing of a quantitative relationship between the gentamicin toxicity and anti-apoptotic modulators will be the first step toward safer gentamicin usage. The possibility of safer gentamicin usage is already indicated, rather empirically. Many compounds have been shown to attenuate the gentamicin effect. The effects of sesame oil, vitamin E and N-acetyl cysteine have been explained on the basis of their anti-oxidative functions [40, 41]. Knauer et al. provided the first evidence that the apoptosis inhibitor protein survivin protects the auditory system from gentamicin toxicity [42]. Leptin (PI3K-Akt signaling pathway modulator) and flunarizine (mitochondrial permeability transition pore inactivator) have also been shown to be reno-protective following gentamicin treatment [43, 44]. All apoptotic attenuating compounds are expected to attenuate gentamicin induced nephrotoxicity. The proposed mechanism of gentamicin toxicity places these experimental observations in proper perspective.

Conclusions

Binding of gentamicin to calreticulin is modeled and compared with the crystal structure of the complex of calreticulin with Glc_1Man_3 tetrasaccharide. The details of the interactions and the participating residues help in understanding the structural similarity between the binding of the two molecules.

Gentamicin could be a potential competitive inhibitor that binds to the lectin site of calreticulin molecule. The implications of such an inhibition are described.

Acknowledgments The 'Pool Officer fellowship' to GH from the Council of Scientific and Industrial Research is acknowledged. The financial support given to the Biomedical Informatics Center at the institute by the Indian Council of Medical Research, Government of India, is gratefully acknowledged.

References

1. Rea RS, Capitano B (2007) Semin Respir Crit Care Med 28:596–603
2. Durante-Mangoni E, Grammatikos A, Utili R, Falagas ME (2009) Int J Antimicrob Agents 33:201–205
3. Davies J, Davis BD (1968) J Biol Chem 243:3312–3316
4. Oliveira JF, Silva CA, Barbieri CD, Oliveira GM, Zanetta DM et al. (2009) Antimicrob Agents Chemother 53:2887–2891
5. Quiros Y, Vicente-Vicente L, Morales AI, López-Novoa JM, López-Hernández FJ (2011) Toxicol Sci 119:245–256
6. Martínez-Salgado C, López-Hernández FJ, López-Novoa JM (2007) Toxicol Appl Pharmacol 223:86–98
7. Servais H, Ortiz A, Devuyst O, Denamur S, Tulkens PM et al. (2008) Apoptosis 13:11–32
8. Walker PD, Barri Y, Shah SV (1999) Ren Fail 21:433–442
9. Whelton A (1979) Prog Clin Biol Res 35:33–41
10. Morales AI, Arévalo M, Pérez-Barriocanal F (2000) Nefrologia 20:408–414
11. Horibe T, Matsui H, Tanaka M, Nagai H, Yamaguchi Y et al. (2004) Biochem Biophys Res Commun 323:281–287
12. Balakumar P, Rohilla A, Thangathirupathi A (2010) Pharmacol Res 62:179–186
13. Koslov G, Pocanschi CL, Rosenauer A, Bastos-Aristizabal S, Gorelik A et al. (2010) J Biol Chem 285:38612–38620
14. Accelrys Software Inc (2003) Cerius2 modeling environment, release 4.7. Accelrys Software Inc, San Diego
15. Brooks BR, Bruccoleri RE, Olafson BD, States DJ, Swaminathan S, Karplus M (1983) J Comput Chem 4:187–217
16. Momany FA, Rone R (1992) J Comput Chem 13:888–900
17. Halgren TA (1996) J Comput Chem 17:490–519
18. Venkatachalam CM, Jiang X, Oldfield T, Waldman M (2003) J Mol Graph Model 21:289–307
19. Mayo SL, Olafson BD, Goddard WA III (1990) J Phys Chem 94:8897–8909
20. Krammer A, Kirchhoff PD, Jiang X, Venkatachalam CM, Waldman M (2005) J Mol Graph Model 23:395–407
21. Sönnichsen B, Füllekrug J, Van Nguyen P, Diekmann W, Robinson DG, Mieskes G (1994) J Cell Sci 107:2705–2717
22. Ware FE, Vassilakos A, Peterson PA, Jackson MR, Lehrman MA, Williams DB (1995) J Biol Chem 270:4697–4704
23. Spiro RG, Zhu Q, Bhoyroo V, Soling HD (1996) J Biol Chem 271:11588–11594
24. Vassilakos A, Cohen Doyle MF, Peterson PA, Jackson MR, Williams DB (1996) EMBO J 15:1495–1506
25. Kapoor M, Srinivas H, Kandiah E, Gemma E, Ellgaard L et al. (2003) J Biol Chem 278:6194–6200
26. Thomson SP, Williams DB (2005) Cell Stress Chaperones 10:242–251
27. Gopalakrishnapai J, Gupta G, Karthikeyan T, Sinha S, Kandiah E et al. (2006) Biochem Biophys Res Commun 351:14–20
28. Kapoor M, Ellgaard L, Gopalakrishnapai J, Schirra C, Gemma E et al. (2004) Biochemistry 43:97–106
29. Schrag JD, Bergeron JJ, Li Y, Borisova S, Hahn M et al. (2001) Mol Cell 8:633–644
30. Das U, Hariprasad G, Ethayathulla AS, Manral P, Das TK et al. (2007) PLoS One 2:e1176
31. Kaufman RJ (1999) Genes Dev 13:1211–1233
32. Malhotra JD, Kaufman RJ (2007) Antioxid Redox Signal 9:2277–2293
33. Yoshida H (2007) FEBS J 274:630–658
34. Kitamura M (2008) Clin Exp Nephrol 12:317–325
35. Peyrou M, Hanna PE, Cribb AE (2007) Toxicol Sci 99:346–353
36. Tablan OC, Reyes MP, Rintelmann WF, Lerner AM (1984) J Infect Dis 149:257–263
37. Gregersen N, Bross P (2010) Mol Biol 648:3–23
38. Miyazaki T, Sagawa R, Honma T, Noguchi S, Harada T, Komatsuda A et al. (2004) J Biol Chem 279:17295–17300
39. Yamamoto S, Nakano S, Owari K, Fuziwara K, Ogawa N et al. (2010) FEBS Lett 584:645–651
40. Hsu DZ, Li YH, Chu PY, Periasamy S, Liu MY (2011) Antimicrob Agents Chemother 55:2532–2536
41. Patel MB, Deshpande S, Shah G (2011) Ren Fail 33:341–347
42. Knauer SK, Heinrich UR, Bier C, Habtemichael N, Docter D et al. (2010) Cell Death Dis 1e51
43. Chen YC, Chen CH, Hsu YH, Chen TH, Sue YM et al. (2011) Eur J Pharmacol 658:213–218
44. Muthuraman A, Singla SK, Rana A, Singh A, Sood S (2011) Yakugaku Zasshi 131:437–443